High-Resolution Finite Volume Methods with Application to Volcano and Tsunami Modeling

Randall J. LeVeque
Department of Applied Mathematics
University of Washington

Outline

- Volcanic flows, ash plumes, pyroclastic flow
- Tsunami modeling, shallow water equations

- Finite volume methods for hyperbolic equations
- Conservation laws and source terms
- Riemann problems and Godunov's method
- Wave propagation form
- Wave limiters and high-resolution methods
- Software: CLAWPACK

Some collaborators

Algorithms, software

Marsha Berger, NYU
Donna Calhoun, UW
Phil Colella, UC-Berkeley
Jan Olav Langseth, Oslo
Sorin Mitran, UNC
James Rossmanith, Michigan
Derek Bale, eV Products

Tsunamis

David George, UW
Harry Yeh, OSU

Volcanos

Marica Pelanti, UW
Roger Denlinger, USGS CVO
Dick Iverson, USGS CVO
Alberto Neri, Pisa
T. E. Ongaro, Pisa

Supported in part by NSF and the DOE SciDAC program

Marica Pelanti, Donna Calhoun, Joe Dufek, and David George

at Mount St. Helens

Volcanic fbws

- Flow of magma in conduit
- Little dissolved gas $\Longrightarrow$ lava flows
- Dissolved gas expansion $\Longrightarrow$ phase transition, ash jet
- Ash plumes, Plinian columns
- Collapsing columns, pyroclastic flows or surges
- Lahars (mud flows)
- Debris flows

Volcanic Ash Plumes

Pyroclastic Flows

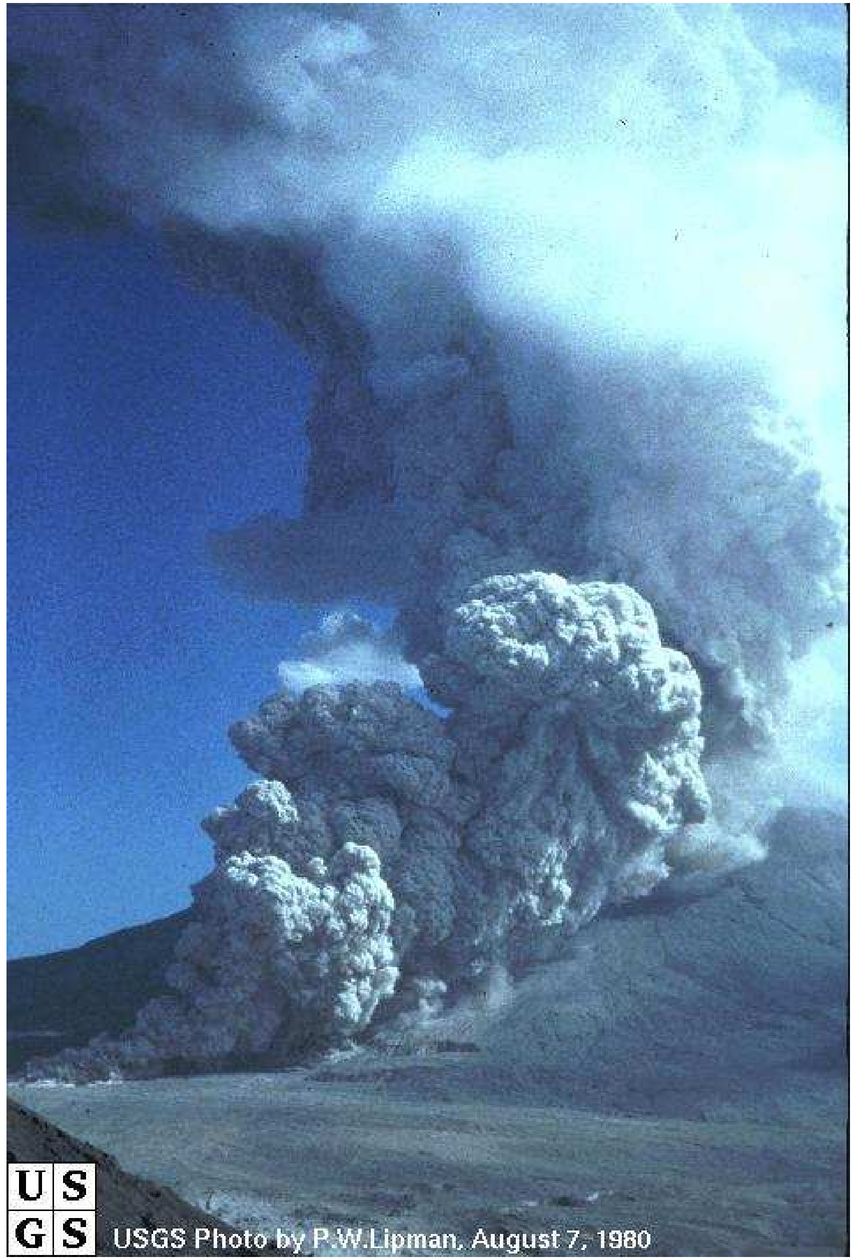

I. Pyroclastic dispersion dynamics of pressure-balanced eruptions

Influence of the diameter D_v and the exit velocity v_v

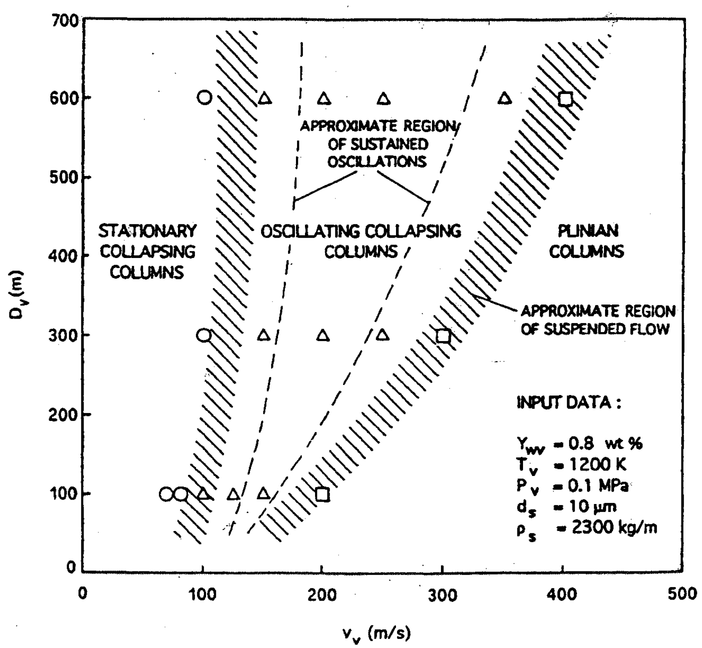

Regions of different types of eruption columns (Neri–Dobran, 1994).

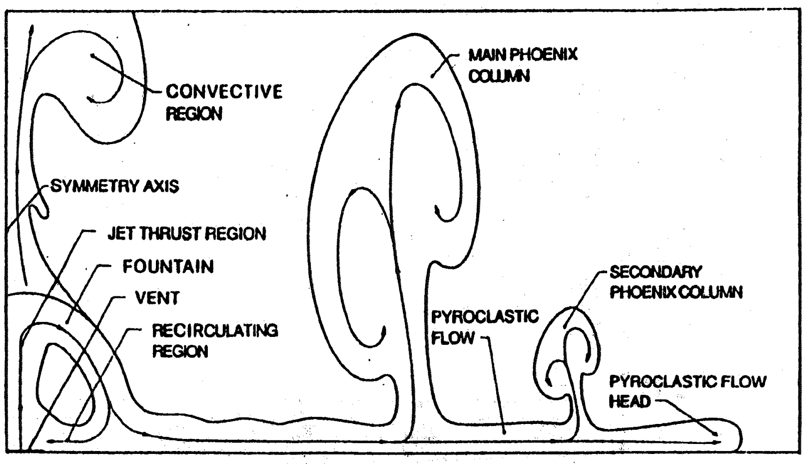

Characteristic features of a collapsing column.

Pyroclastic dispersion dynamics

Vent conditions and physical properties [Neri–Dobran, 1994]:

p_v [MPa]	T_v [K]	α_{dv}	d [μm]	ρ_d [kg/m^3]
0.1	1200	0.01	10	2300

Gas and dust in thermal and mechanical equilibrium at the vent.

Test 1. $D_v = 100\,\mathrm{m}$, $v_v = 80\,\mathrm{m/s}$. $\rightarrow$ Collapsing volcanic column

Test 2. $D_v = 100\,\mathrm{m}$, $v_v = 200\,\mathrm{m/s}$. $\rightarrow$ Transitional/Plinian column

Numerical Experiments

Injection of a hot supersonic particle-laden gas
from a volcanic vent into a cooler atmosphere.

- ⋆ Initially: Standard atmosphere vertically stratified in pressure and temperature all over the domain;
- ⋆ At the vent: Gas pressure, velocities, temperatures, volumetric fractions of gas and dust assumed to be fixed and constant;
- ⋆ Ground boundary: modeled as a free-slip reflector;
- ⋆ Other boundaries:

  2D experiments: Axisymmetric configuration. Symmetry axis: free-slip reflector; Upper and right-hand edges of the domain: free flow boundaries (all the variables gradients set to zero).

  Fully 3D experiments: Upper and lateral sides: free-flow boundaries.

$D_v = 100\,\mathrm{m}$, $v_v = 80\,\mathrm{m/s}$. Collapsing column.

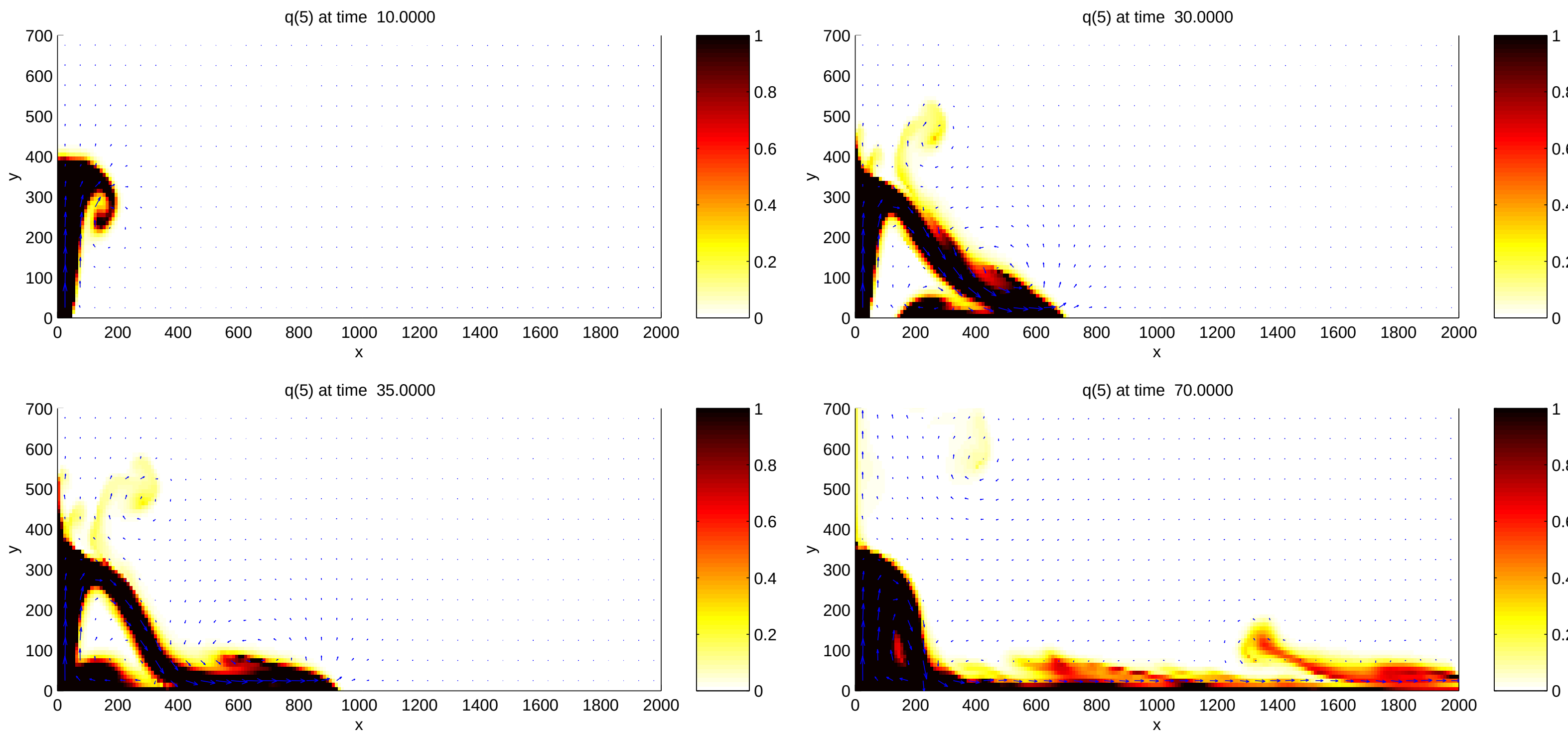

Dust density at $t = 10, 30,\ 35,\ 70$ s. Uniform grid, 200×100 cells. Cell size = 10 m. CFL = 0.9.

Physical Model

Two-phase fluid flow composed of solid particles (dust) in a gas.

Gas phase: compressible;
Dust phase: incompressible (constant microscopic mass density ρ_d).

Dust particles are assumed to be dispersed (vol. fraction $\alpha_d \ll 1$), with negligible particle-particle interaction. The solid phase is thus considered pressureless.

Model accounts for:

- Gravity;
- Interphase drag force;
- Interphase heat transfer.

Some of the neglected phenomena: viscous stress, turbulence.

Model Equations

Conservation of mass, momentum, and energy for gas and dust

$$\rho_t + \nabla \cdot (\rho \mathbf{u}_g) = 0\,,$$

$$(\rho \mathbf{u}_g)_t + \nabla \cdot (\rho \mathbf{u}_g \otimes \mathbf{u}_g + p\mathbf{I}) = \rho \mathbf{g} - D(\mathbf{u}_g - \mathbf{u}_d)\,,$$

$$E_t + \nabla \cdot ((E + p)\mathbf{u}_g) = \rho \mathbf{u}_g \cdot \mathbf{g} - D(\mathbf{u}_g - \mathbf{u}_d) \cdot \mathbf{u}_d - Q(T_g - T_d)\,,$$

$$\beta_t + \nabla \cdot (\beta \mathbf{u}_d) = 0\,,$$

$$(\beta \mathbf{u}_d)_t + \nabla \cdot (\beta \mathbf{u}_d \otimes \mathbf{u}_d) = \beta \mathbf{g} + D(\mathbf{u}_g - \mathbf{u}_d)\,,$$

$$\Omega_t + \nabla \cdot (\Omega \mathbf{u}_d) = \beta \mathbf{u}_d \cdot \mathbf{g} + D(\mathbf{u}_g - \mathbf{u}_d) \cdot \mathbf{u}_d + Q(T_g - T_d)\,.$$

α_g, α_d = volume fractions ($\alpha_g + \alpha_d = 1$, $\alpha_d \ll 1$);
ρ_g, ρ_d = material mass densities (ρ_d = const.); $\rho = \alpha_g \rho_g$, $\beta = \alpha_d \rho_d$ = macroscopic densities;
$\mathbf{u}_g$, $\mathbf{u}_d$ = velocities; p_g = gas pressure, $p = \alpha_g p_g$;
e_g, e_d = specific total energies, $E = \alpha_g \rho_g e_g$, $\Omega = \alpha_d \rho_d e_d$;
$e_g = \epsilon_g + \frac{1}{2}||\mathbf{u}_g||^2$, $e_d = \epsilon_d + \frac{1}{2}||\mathbf{u}_d||^2$; ϵ_g, ϵ_d = specific internal energies; T_g, T_d = temperatures;
$\mathbf{g} = (0, 0, -g)$ = gravity acceleration (z direction), $g = 9.8\,\mathrm{m/s}^2$;
D = drag function; Q = heat transfer function.

Closure Relations

Gas equation of state: $p_g = (\gamma - 1)\rho_g \epsilon_g \,, \quad \gamma = c_{pg}/c_{vg} = \text{const.};$

Dust energy relation: $\epsilon_d = c_{vd} T_d \,, \quad c_{vd} = \text{const.};$

Drag

$$D = \frac{3}{4} C_{\rm d} \frac{\beta \rho}{\rho_d d} ||\mathbf{u}_g - \mathbf{u}_d|| \,,$$

d = dust particle diameter, $C_{\rm d}$ = drag coefficient,

$$C_{\rm d} = \begin{cases} \frac{24}{Re}\left(1 + 0.15 Re^{0.687}\right) & \text{if } Re < 1000 \,, \\ 0.44 & \text{if } Re \geq 1000 \,, \end{cases}$$

Re = Reynolds number = $\frac{\rho\, d ||\mathbf{u}_g - \mathbf{u}_d||}{\mu}$, μ = dynamic viscosity of the gas.

Heat transfer

$$Q = \frac{Nu\, 6 \kappa_g \beta}{\rho_d d^2} \,,$$

Nu = Nusselt number = $2 + 0.65 Re^{1/2} Pr^{1/3}$, Pr = Prandtl number = $\frac{c_{pg}\mu}{\kappa_g}$,
κ_g = gas thermal conductivity.

Shock structure in a supersonic jet

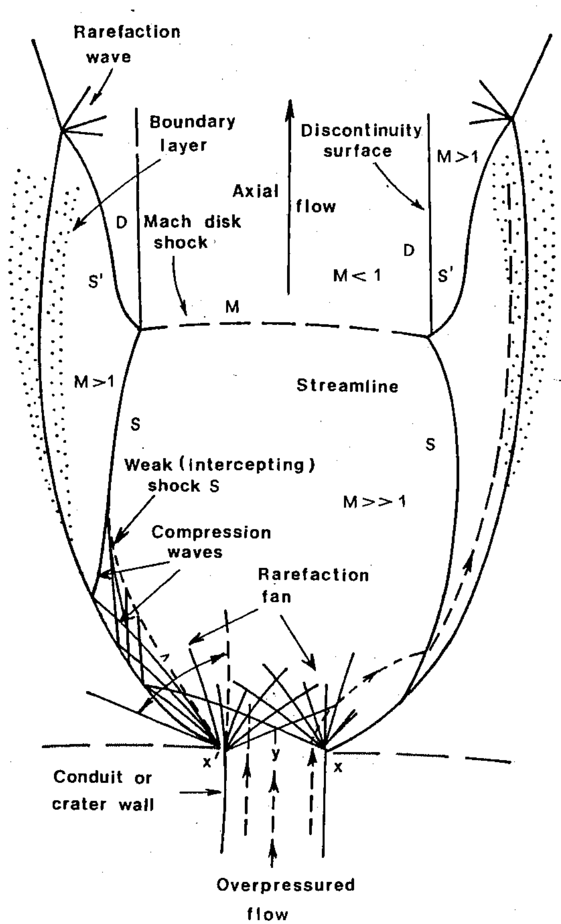

Illustration of an overpressured jet (JANNAF,1975).

Overpressured jet: Mach number and normal Mach number at $t = 30$ s.

No crater $\longrightarrow$

Crater 30° $\longrightarrow$

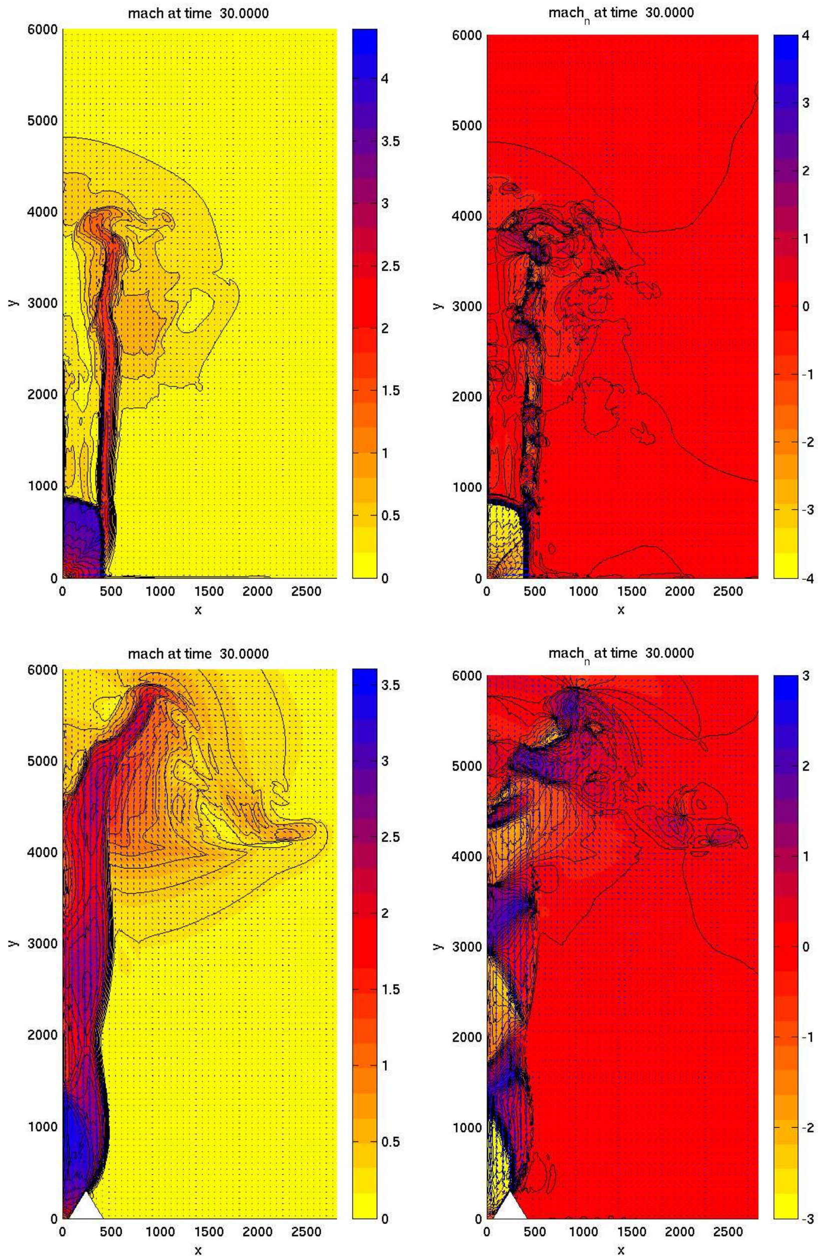

Normal Mach number of the mixture (to highlight normal discontinuities)

$$M_{\mathrm{m}} = \frac{\mathbf{u}_{\mathrm{m}} \cdot \boldsymbol{\nabla} p_g}{c_{\mathrm{m}} || \boldsymbol{\nabla} p_g ||} ,$$

$$c_{\mathrm{m}}^2 = \frac{\rho_g c_g^2}{\alpha_g \rho_{\mathrm{m}}} , \quad c_g = \sqrt{R T_g} ,$$

$$\mathbf{u}_{\mathrm{m}} = \frac{\alpha_g \rho_g \mathbf{u}_g + \alpha_d \rho_d \mathbf{u}_d}{\rho_{\mathrm{m}}} ,$$

$$\rho_{\mathrm{m}} = \alpha_g \rho_g + \alpha_d \rho_d .$$

Comparison: CLAWPACK vs. PDAC2D (Neri–Ongaro, INGV, Pisa, Italy).

No crater

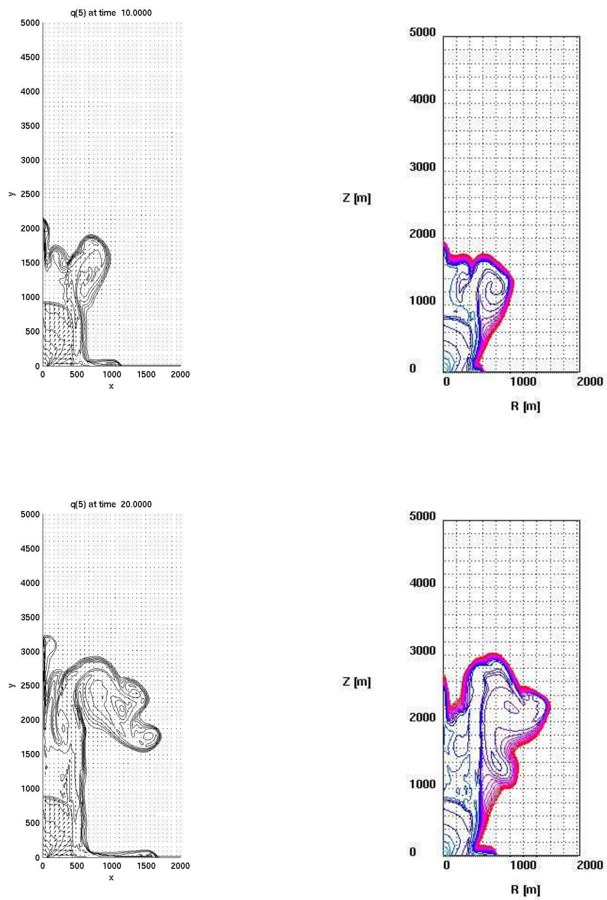

Crater 30°

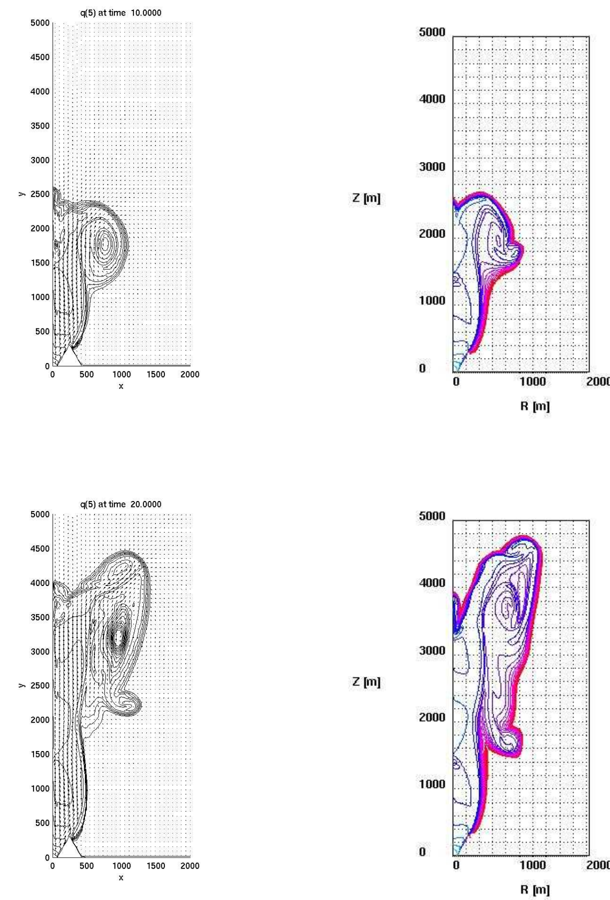

Dust density at at $t = 10$ and 20 s.

Mount St. Helens

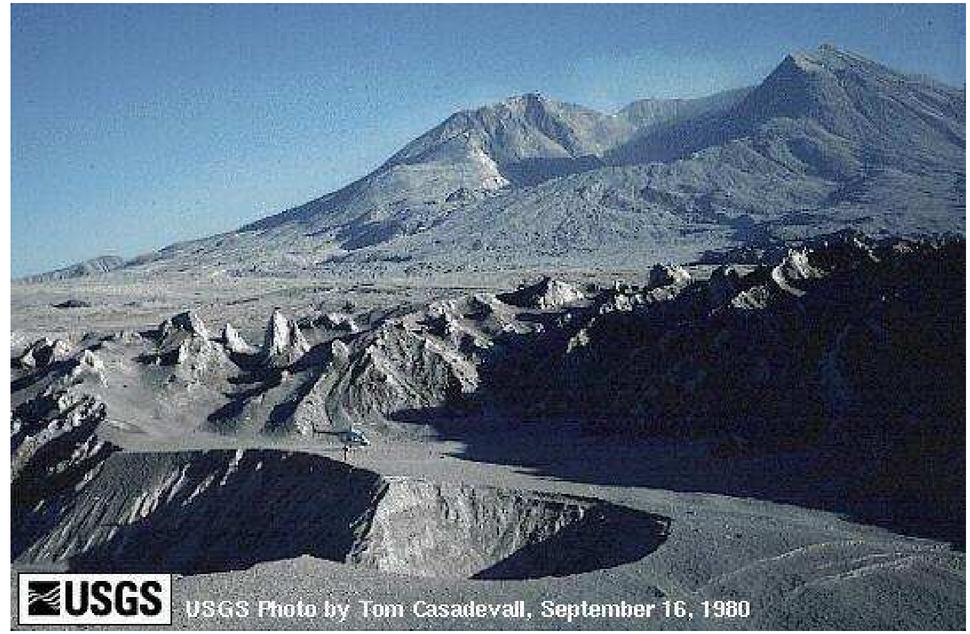

Blast zone at Mount St. Helens

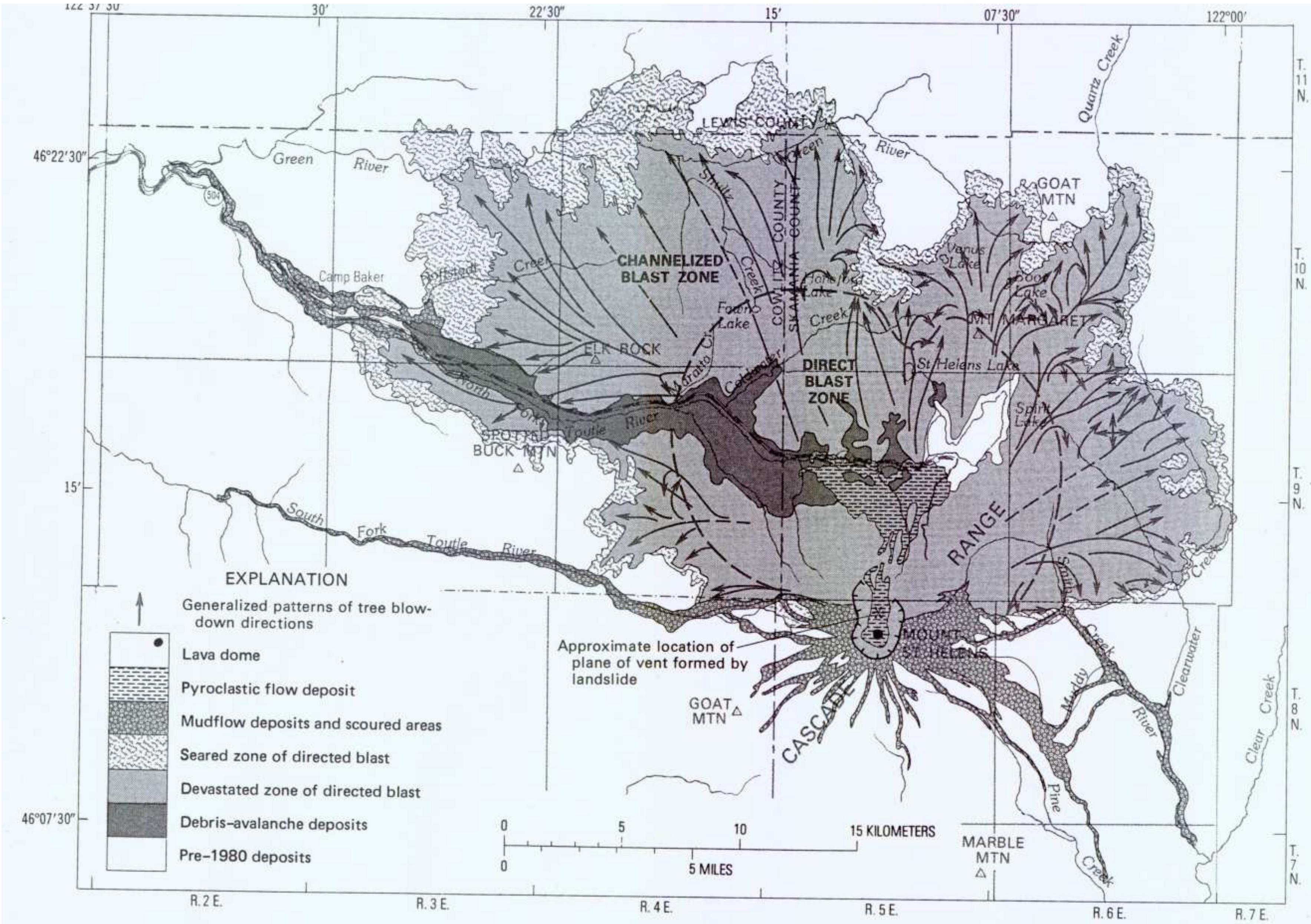

Trees blown down by MSH blast

http://volcanoes.usgs.gov/Hazards/Effects/MSHsurge_effects.

Mount St. Helens

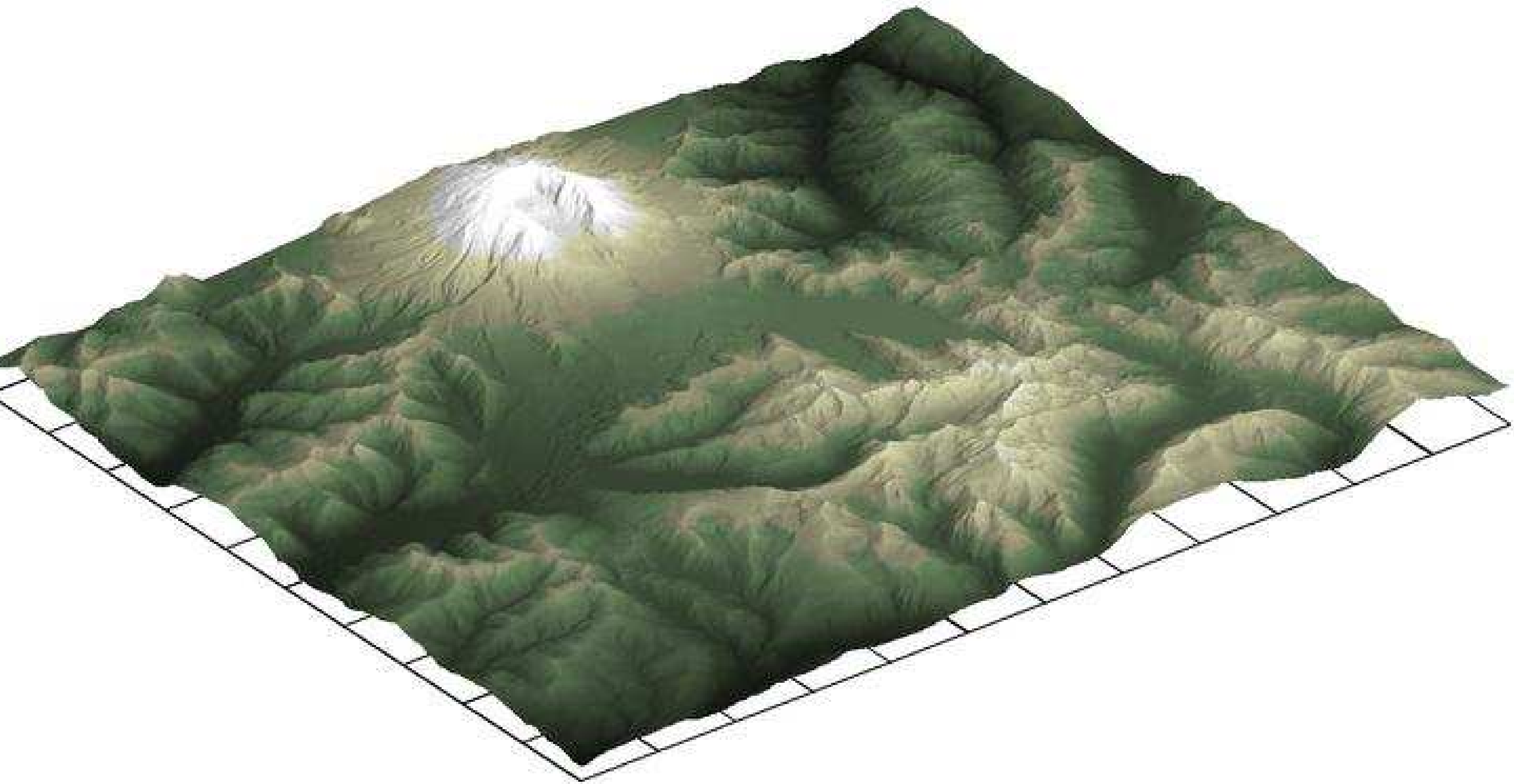

High-pressure initial blast

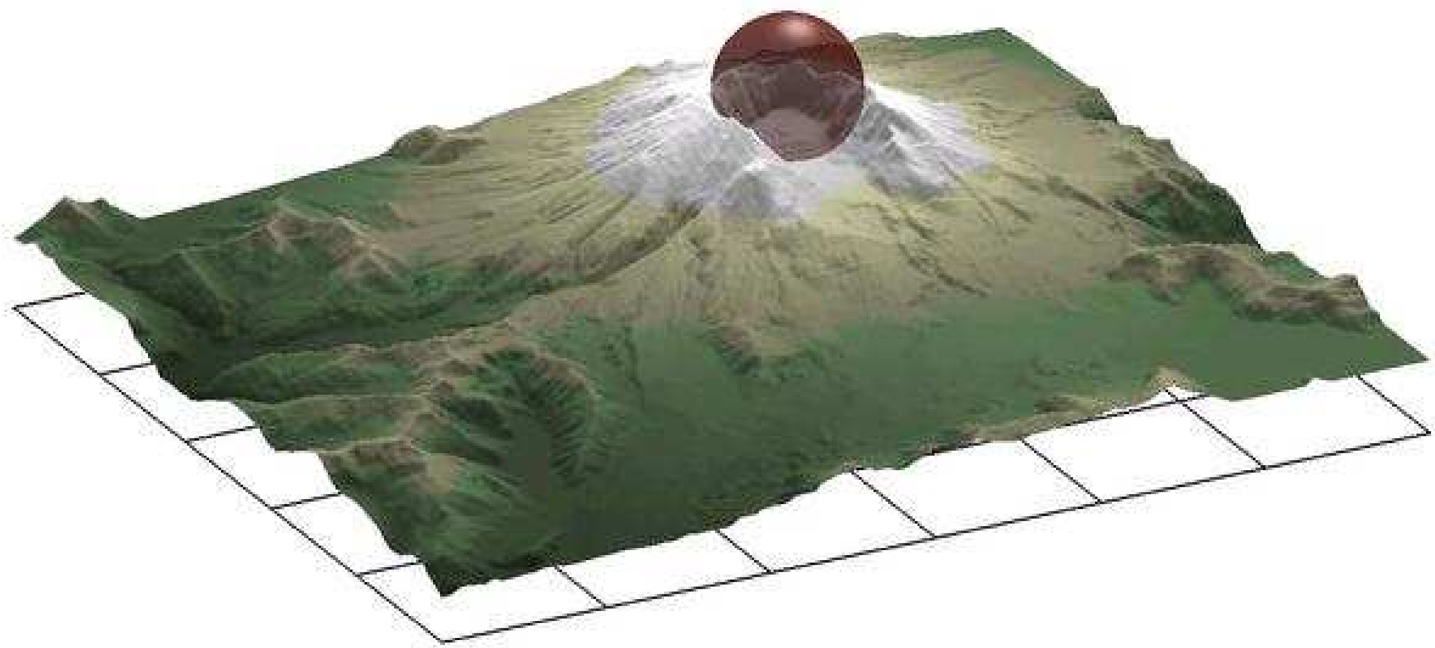

AMR computation

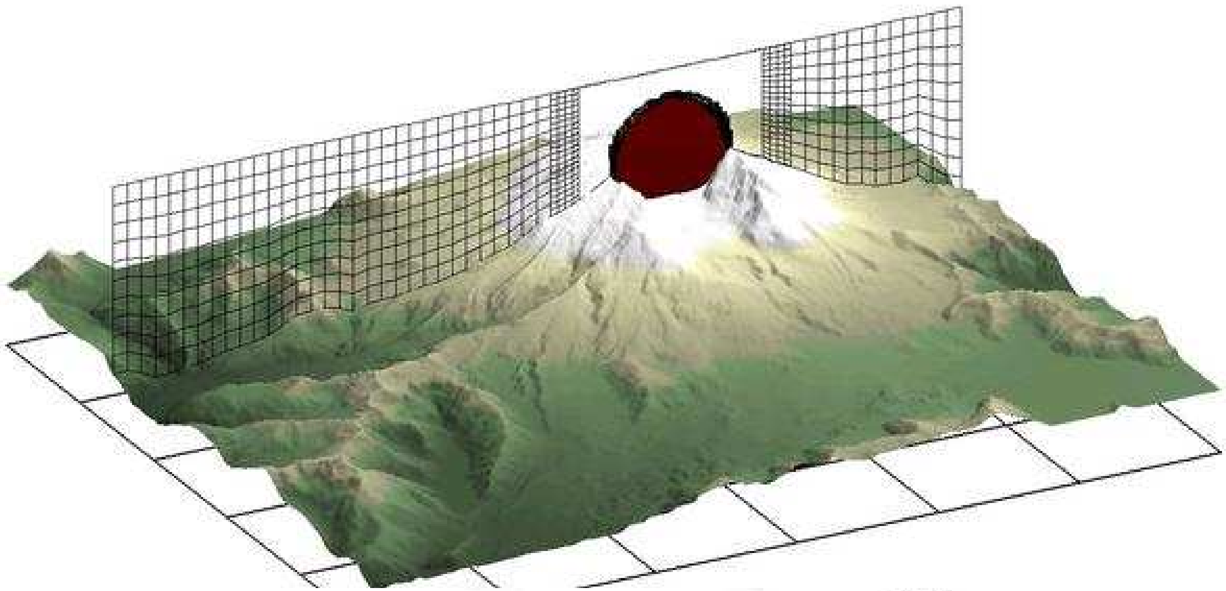

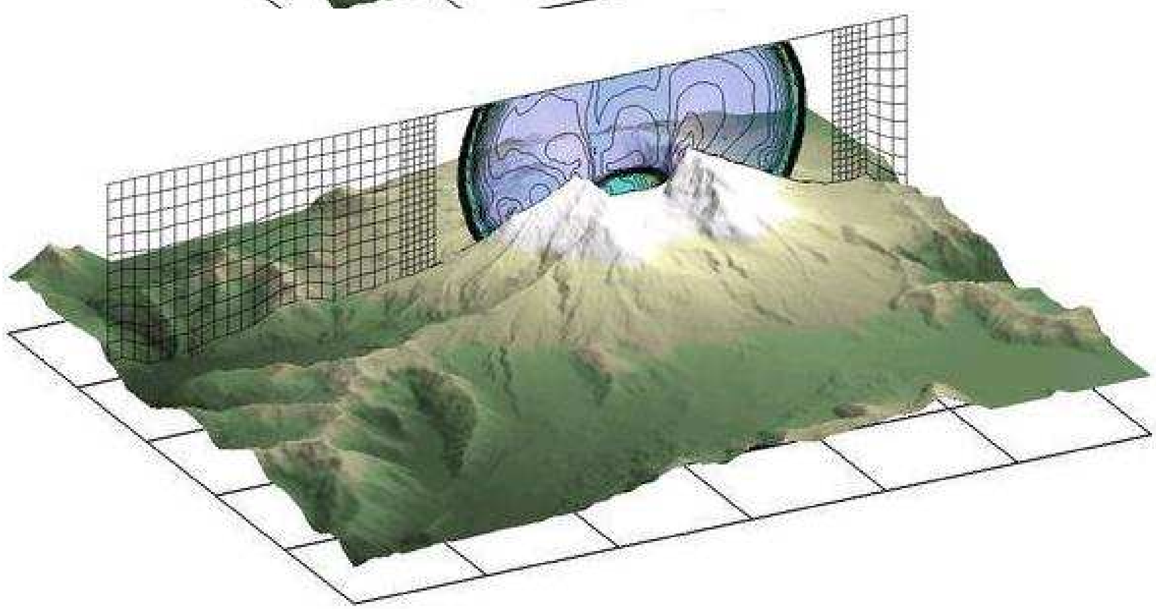

Volcanic Debris Flow

Volcanic Debris Flow

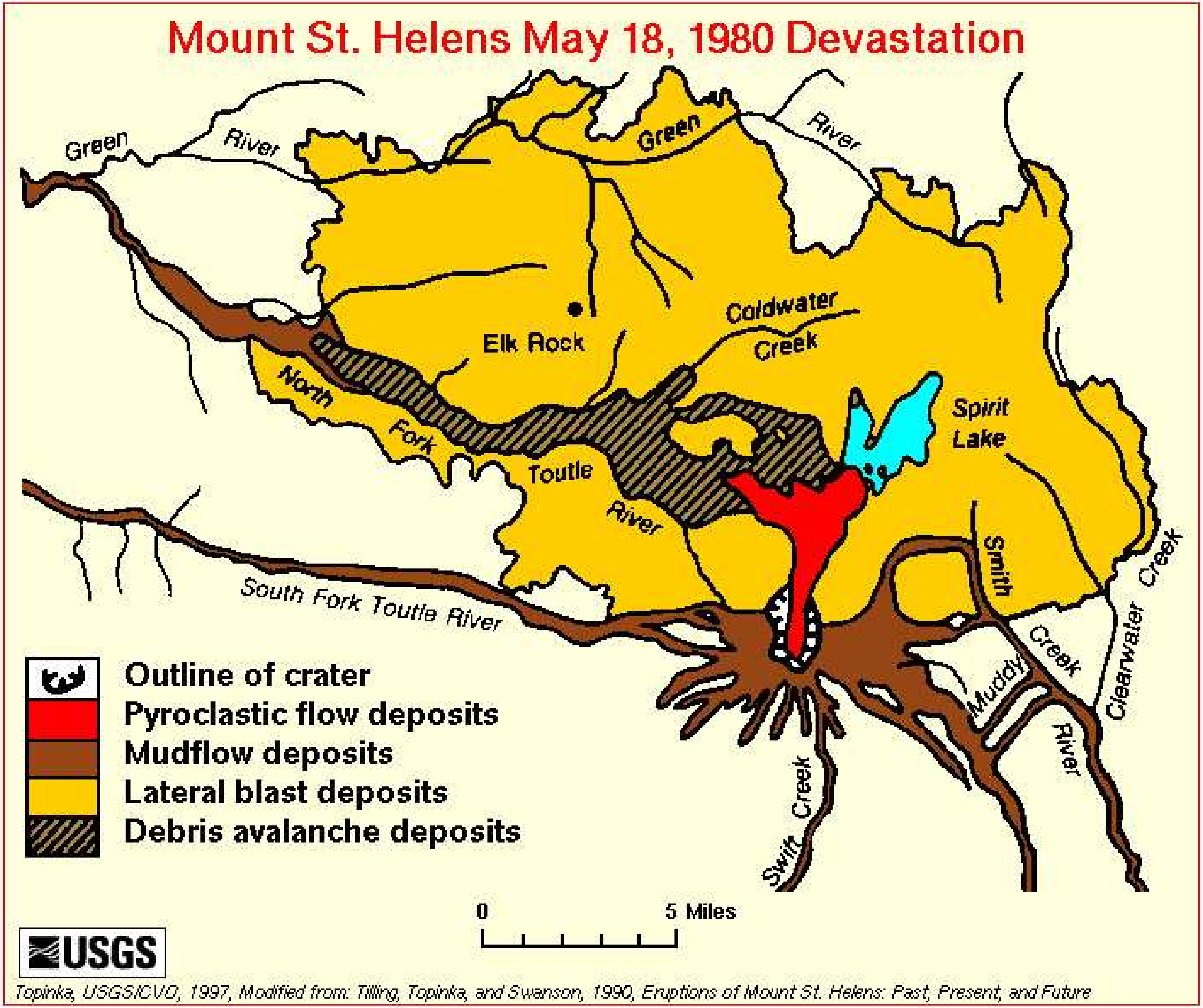

Test flume studies

Cascade Volcano Observatory (CVO), Vancouver, Washington

`http://vulcan.wr.usgs.gov/`

Sand flume with topography

Recent results of Dick Iverson and Roger Denlinger, CVO

Experiments on small-scale sand flume with topography.

Compared to predictions from shallow-flow Savage-Hutter type model for granular avalanches.

Coulomb friction for shear and normal stresses on internal and bounding surfaces.

Finite-volume wave propagation method using finite element computation of stresses in Riemann solver.

Flow over steep topography.

Sand flume with topography

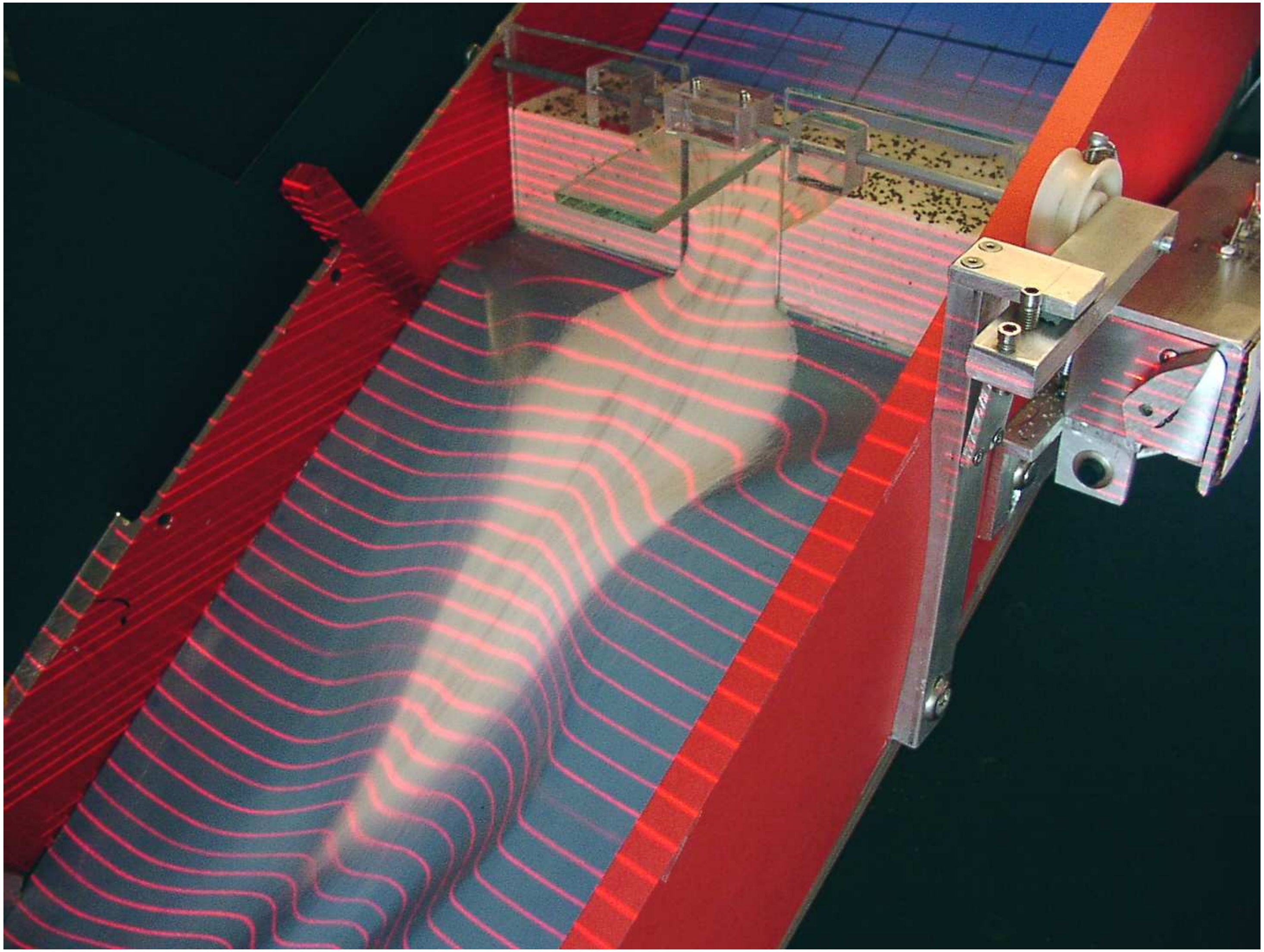

Sand on a flume with topography

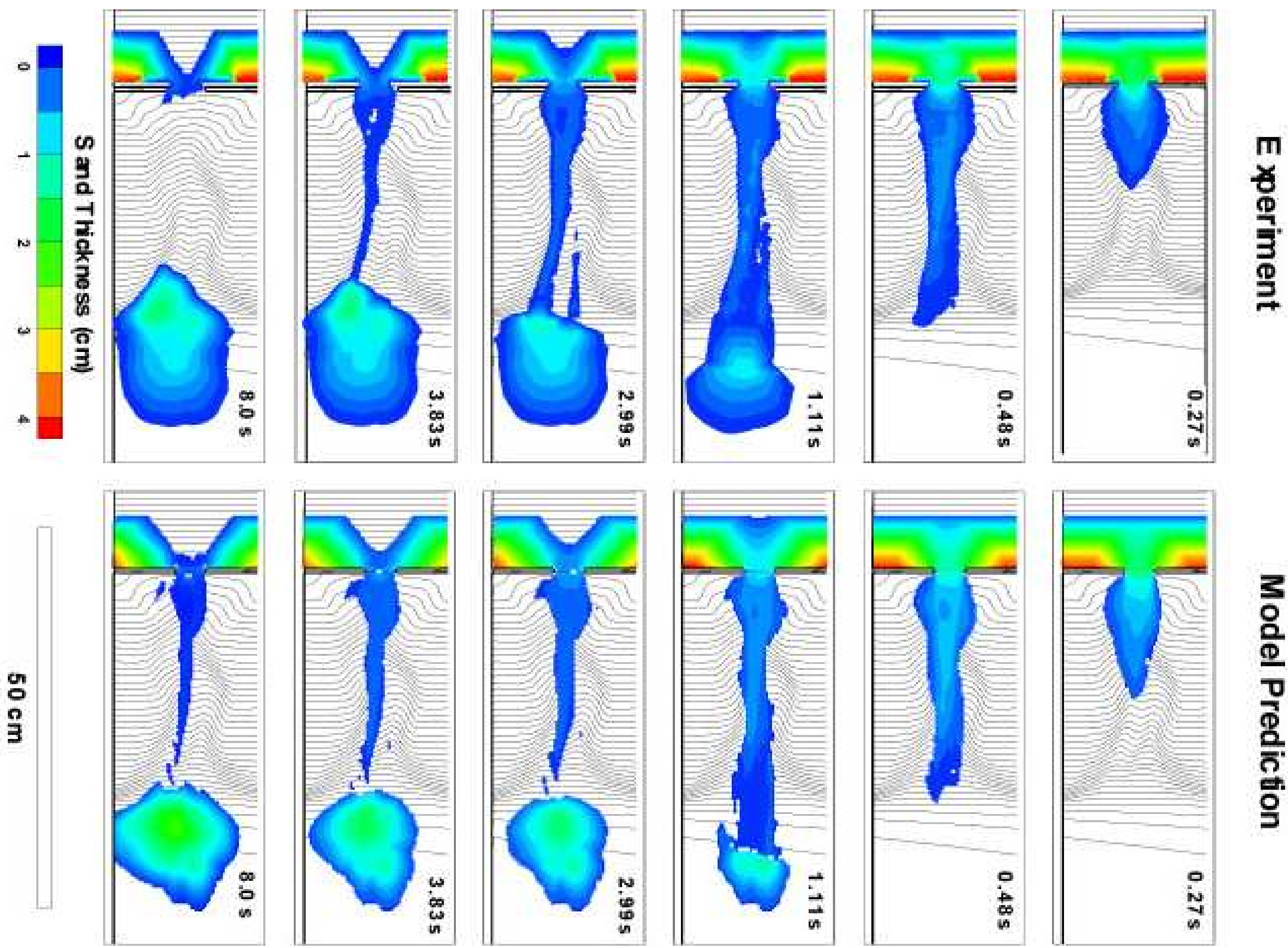

Tsunamis

Generated by

- Earthquakes,
- Landslides,
- Submarine landslides,
- Volcanos,
- Meteorite or asteroid impact

Tsunamis

Generated by

- Earthquakes,
- Landslides,
- Submarine landslides,
- Volcanos,
- Meteorite or asteroid impact

- Small amplitude in ocean (< 1 meter) but can grow to 10s of meters at shore.
- Run-up along shore can inundate 100s of meters inland
- Long wavelength (as much as 200 km)
- Propagation speed $\sqrt{gh}$
- Average depth of Pacific is 4km $\Longrightarrow$ average speed 200 m/s

1993 Okushiri tsunami

http://www.pmel.noaa.gov/tsunami/aerial_photo_okushiri.html

3rd Int'l workshop on long-wave runup models

Benchmark Problem 2:

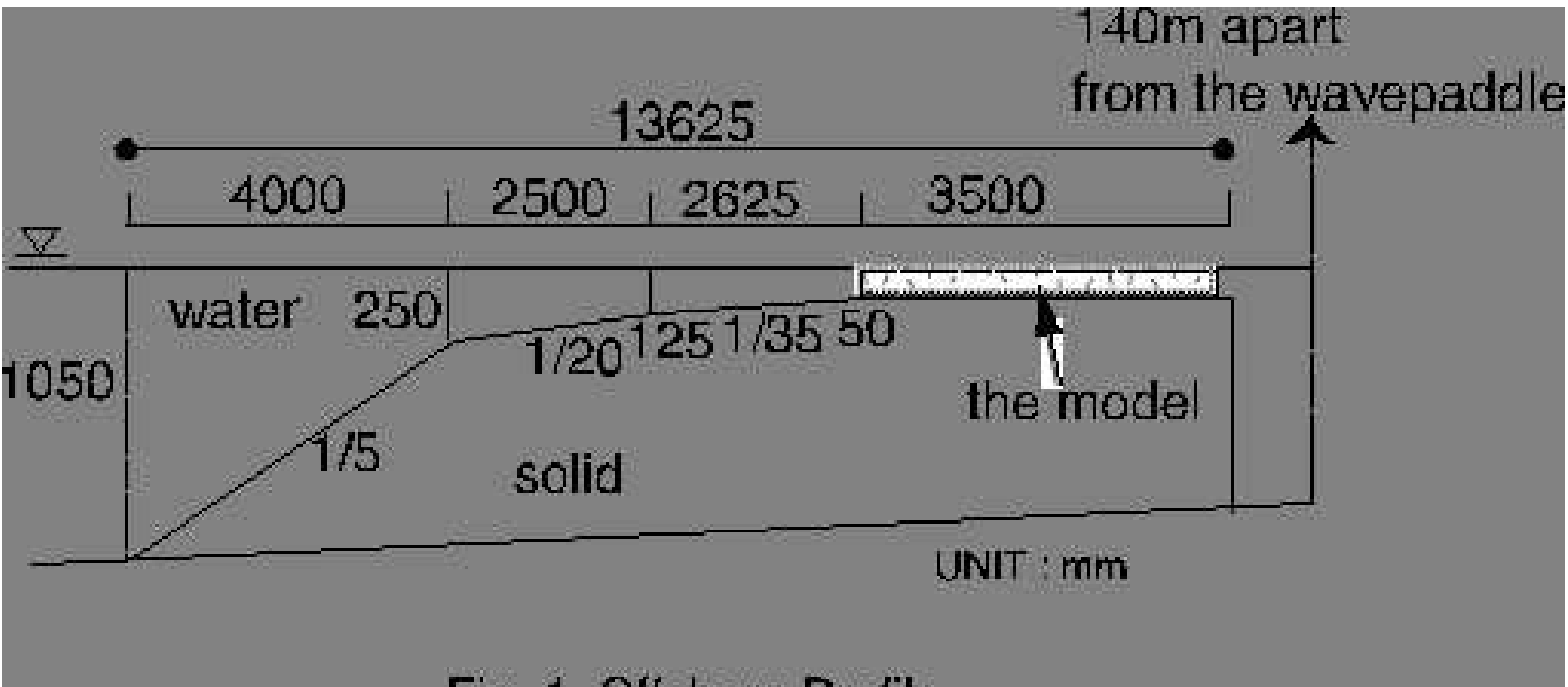

Fig. 1 Offshore Profile

Shallow water equations with topography $B(x, y)$

$$
\begin{aligned}
h_t + (hu)_x + (hv)_y &= 0 \\
(hu)_t + \left(hu^2 + \frac{1}{2}gh^2\right)_x + (huv)_y &= -ghB_x(x, y) \\
(hv)_t + (huv)_x + \left(hv^2 + \frac{1}{2}gh^2\right)_y &= -ghB_y(x, y)
\end{aligned}
$$

Applications:

- Tsunamis
- Estuaries
- River flooding, dam breaks
- Debris flows from volocanic eruptions

Frame 11

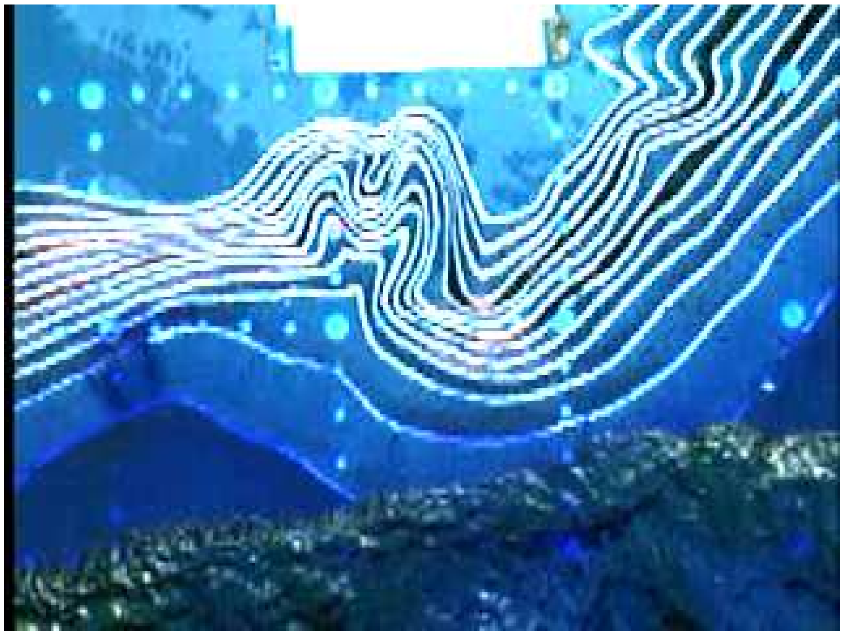

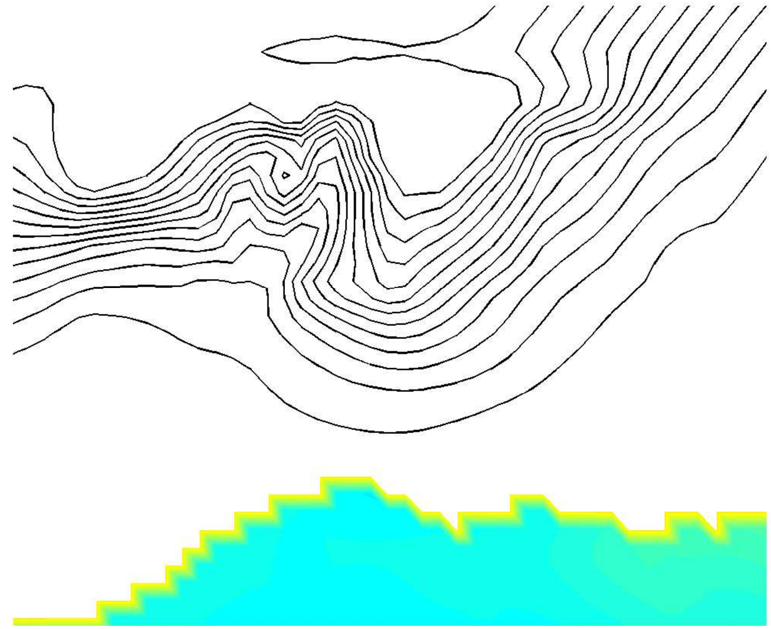

Frame 26

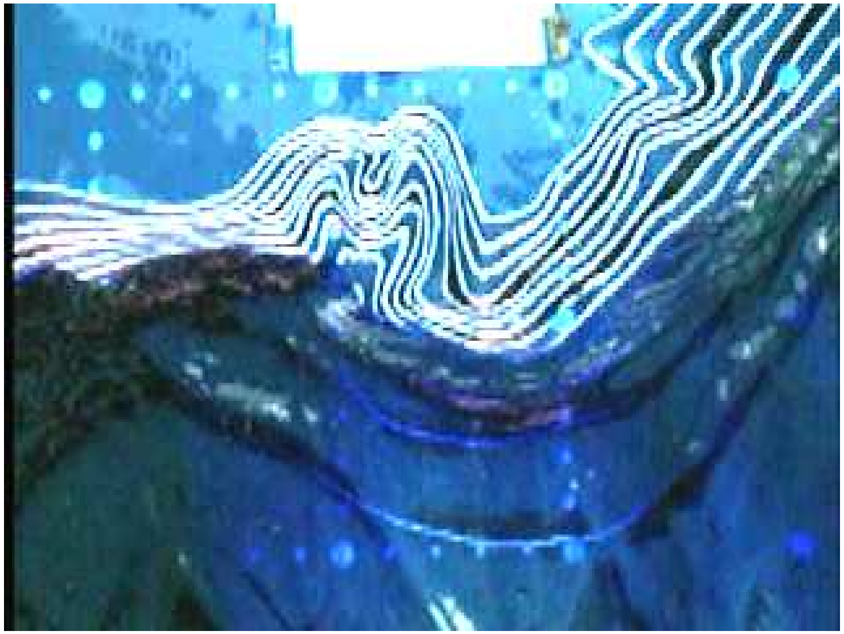

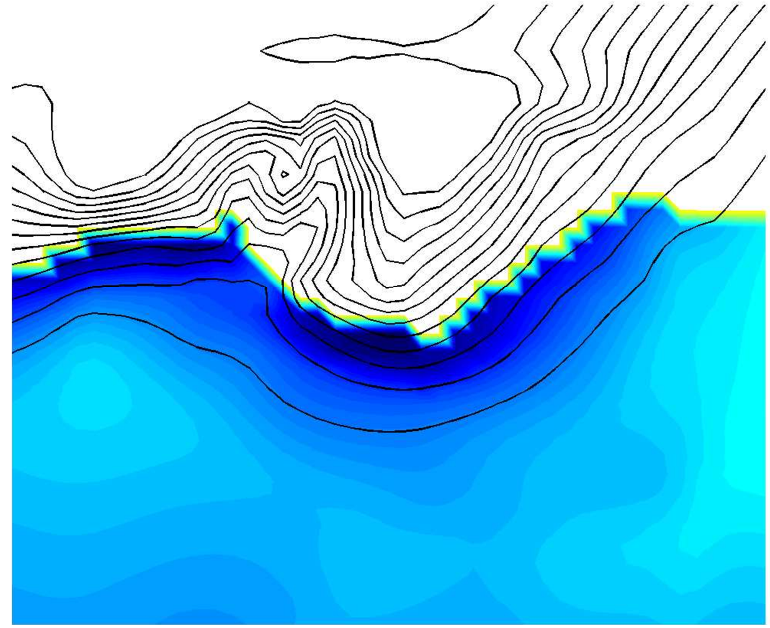

Frame 41

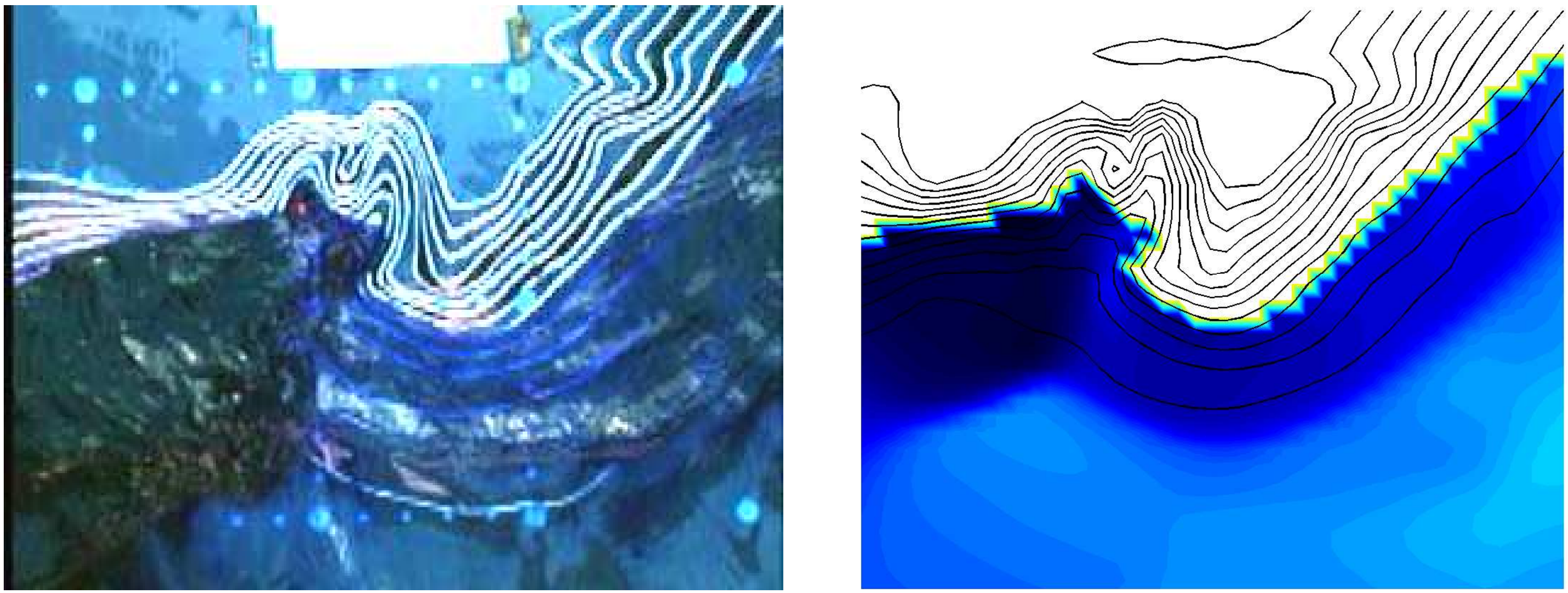

Frame 56

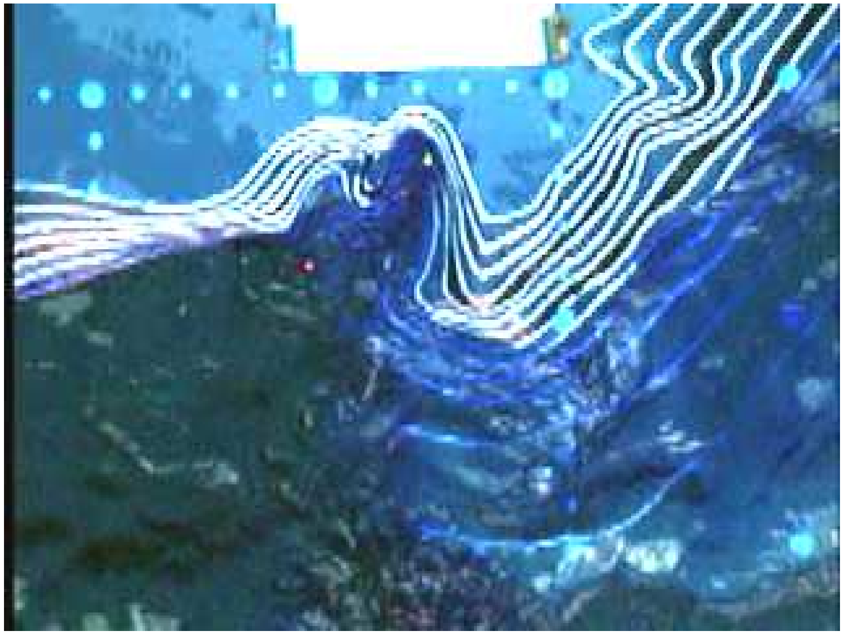

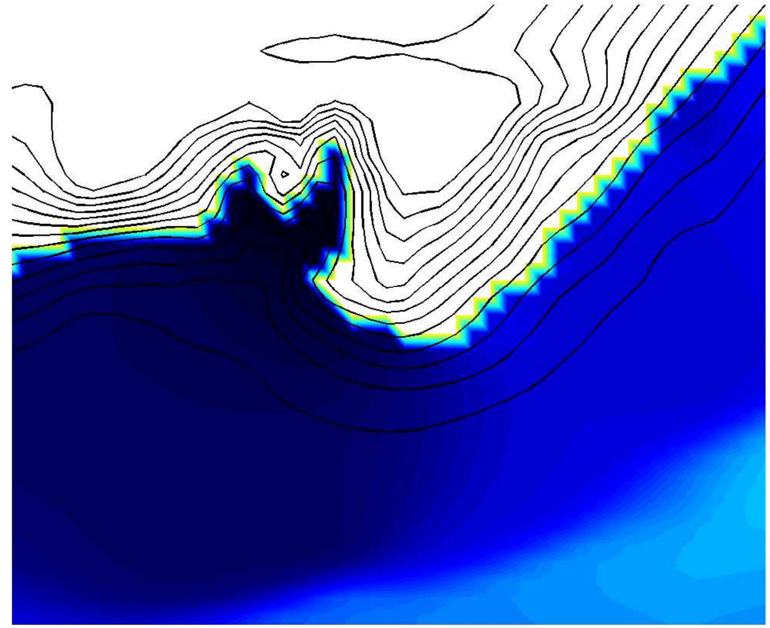

Channel 5

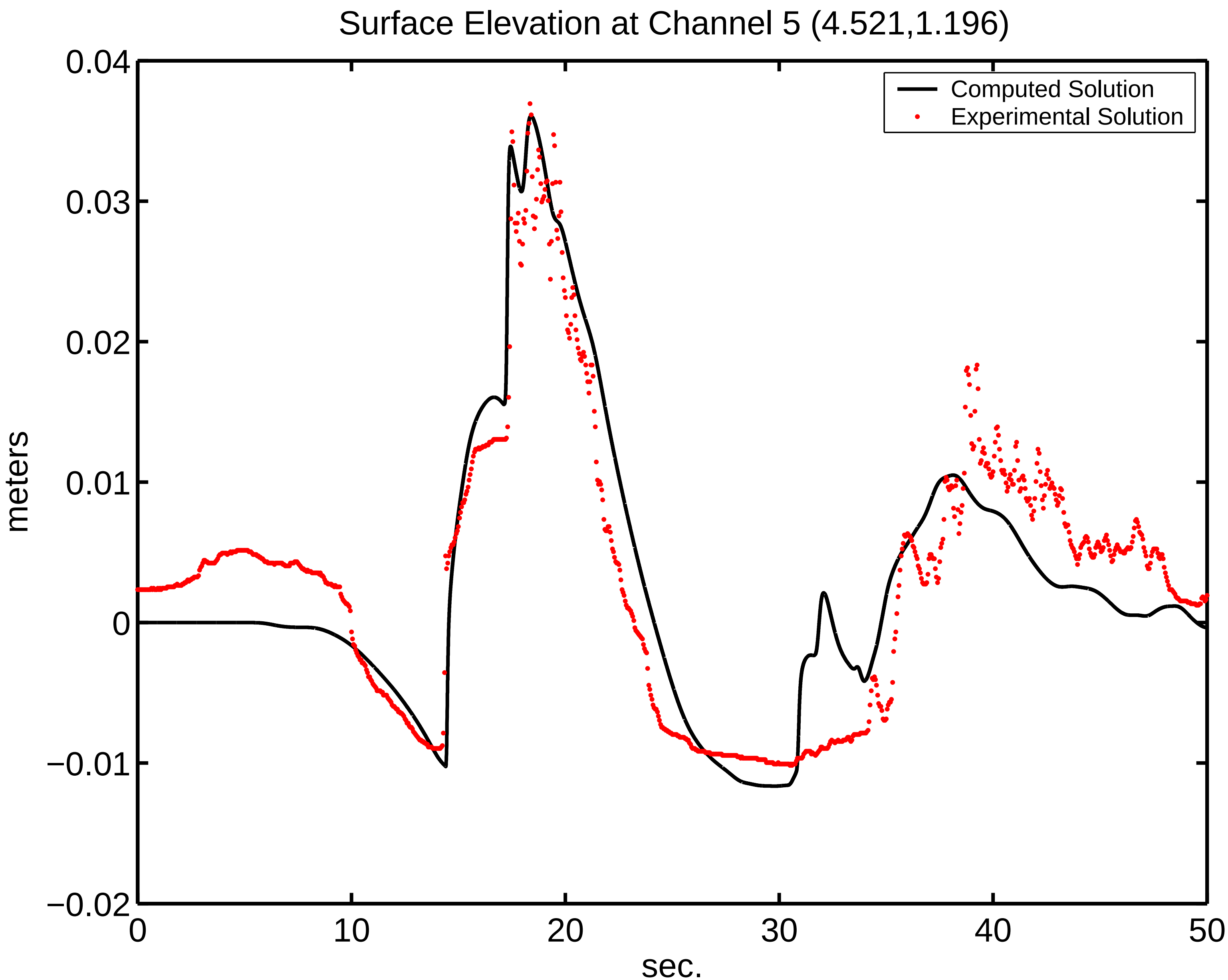

Surface Elevation at Channel 5 (4.521,1.196)
Computed Solution
Experimental Solution
meters
sec.
0.04
0.03
0.02
0.01
0
−0.01
−0.02
0
10
20
30
40
50

Hyperbolic Partial Differential Equations

Model advective transport or wave propagation

Advection equation:

$$q_t + uq_x = 0, \qquad q_t + uq_x + vq_y = 0$$

First-order system:

$$q_t + Aq_x = 0, \qquad q_t + Aq_x + Bq_y = 0$$

where $q \in \mathbb{R}^m$ and $A, B \in \mathbb{R}^{m \times m}$.

Hyperbolic if

1D: A is diagonalizable with real eigenvalues,
2D: $\cos(\theta)A + \sin(\theta)B$ is diagonalizable with real eigenvalues, for all angles θ.

Eigenvalues give wave speeds, eigenvectors the wave forms.

Nonlinear conservation laws

$q_t + f(q)_x = 0$, where $f(q)$ is the flux function.

Quasi-linear form: $q_t + f'(q)q_x = 0$.

Hyperbolic if $f'(q)$ is diagonalizable with real eigenvalues.

Eigenvalues depend on solution

$\Longrightarrow$ characteristics may converge.

$\Longrightarrow$ Shock formation and discontinuous solutions.

Finite-difference Methods

- Pointwise values $Q_i^n \approx q(x_i, t_n)$
- Approximate derivatives by finite differences
- Assumes smoothness

Finite-volume Methods

- Approximate cell averages: $Q_i^n \approx \dfrac{1}{\Delta x} \displaystyle\int_{x_{i-1/2}}^{x_{i+1/2}} q(x, t_n)\, dx$
- Integral form of conservation law,

$$\frac{\partial}{\partial t} \int_{x_{i-1/2}}^{x_{i+1/2}} q(x,t)\, dx \quad = \quad f(q(x_{i-1/2}, t)) - f(q(x_{i+1/2}, t))$$

leads to conservation law $q_t + f_x = 0$ but also directly to numerical method.

Finite volume method

$Q_i^n \approx \frac{1}{\Delta x} \int_{x_{i-1/2}}^{x_{i+1/2}} q(x, t_n)\, dx$

Integral form: $$\frac{\partial}{\partial t} \int_{x_{i-1/2}}^{x_{i+1/2}} q(x,t)\, dx = f(q(x_{i-1/2},t)) - f(q(x_{i+1/2},t))$$

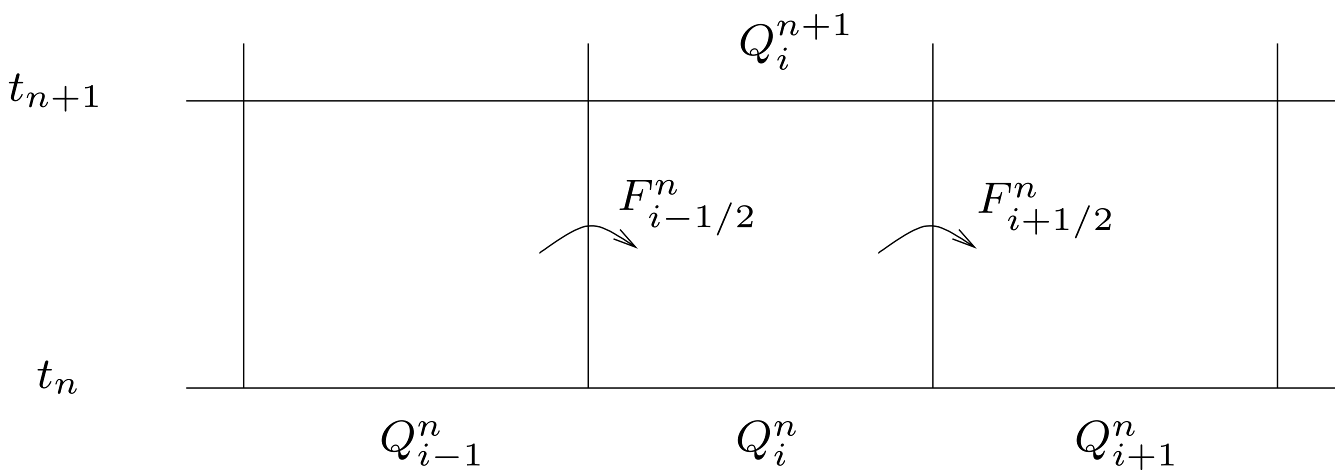

Numerical method: $$Q_i^{n+1} = Q_i^n - \frac{\Delta t}{\Delta x}(F_{i+1/2}^n - F_{i-1/2}^n)$$

Numerical flux: $F\,_{i-1/2}^{\,n} \approx \dfrac{1}{\Delta t} \displaystyle\int_{t_n}^{t_{n+1}} f(q(x_{i-1/2},t))\, dt.$

The Riemann problem

The Riemann problem for $q_t + f(q)_x = 0$ has special initial data

$$q(x,0) = \begin{cases} q_l & \text{if } x < x_{i-1/2} \\ q_r & \text{if } x > x_{i-1/2} \end{cases}$$

Dam break problem for shallow water equations

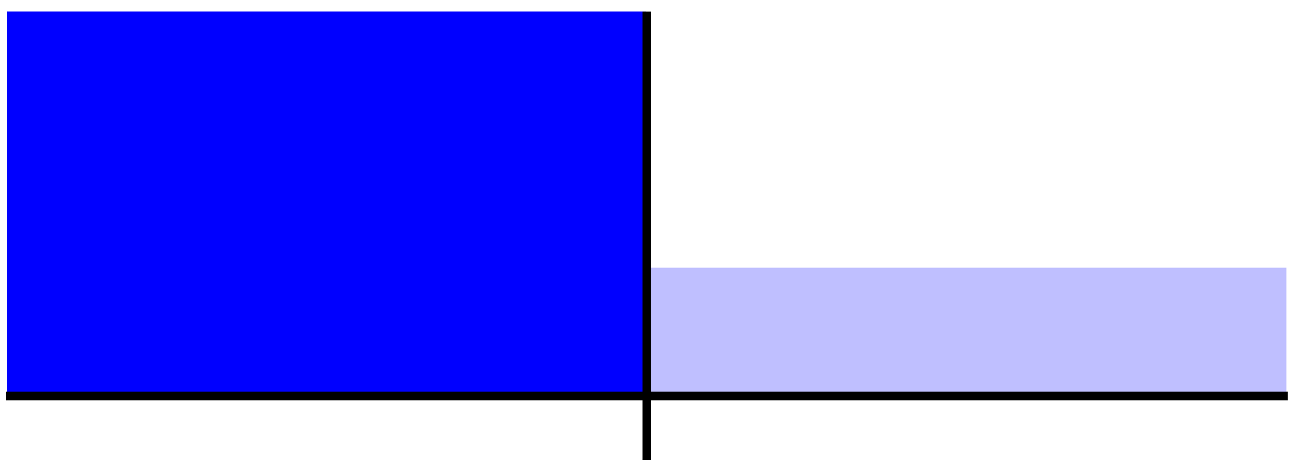

The Riemann problem

The Riemann problem for $q_t + f(q)_x = 0$ has special initial data

$$q(x,0) = \begin{cases} q_l & \text{if } x < x_{i-1/2} \\ q_r & \text{if } x > x_{i-1/2} \end{cases}$$

Dam break problem for shallow water equations

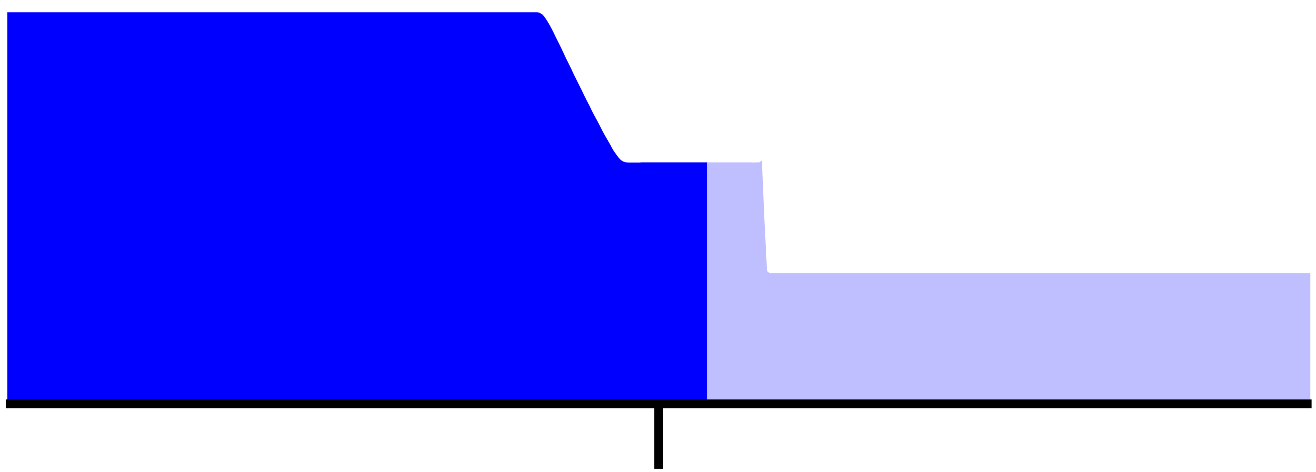

The Riemann problem

The Riemann problem for $q_t + f(q)_x = 0$ has special initial data

$$q(x,0) = \begin{cases} q_l & \text{if } x < x_{i-1/2} \\ q_r & \text{if } x > x_{i-1/2} \end{cases}$$

Dam break problem for shallow water equations

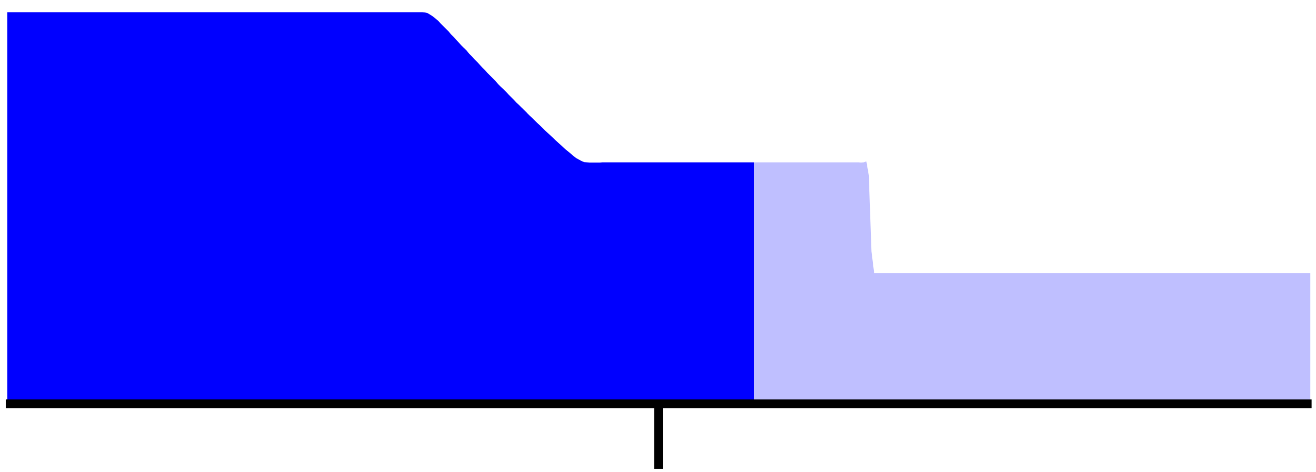

The Riemann problem

The Riemann problem for $q_t + f(q)_x = 0$ has special initial data

$$q(x,0) = \begin{cases} q_l & \text{if } x < x_{i-1/2} \\ q_r & \text{if } x > x_{i-1/2} \end{cases}$$

Dam break problem for shallow water equations

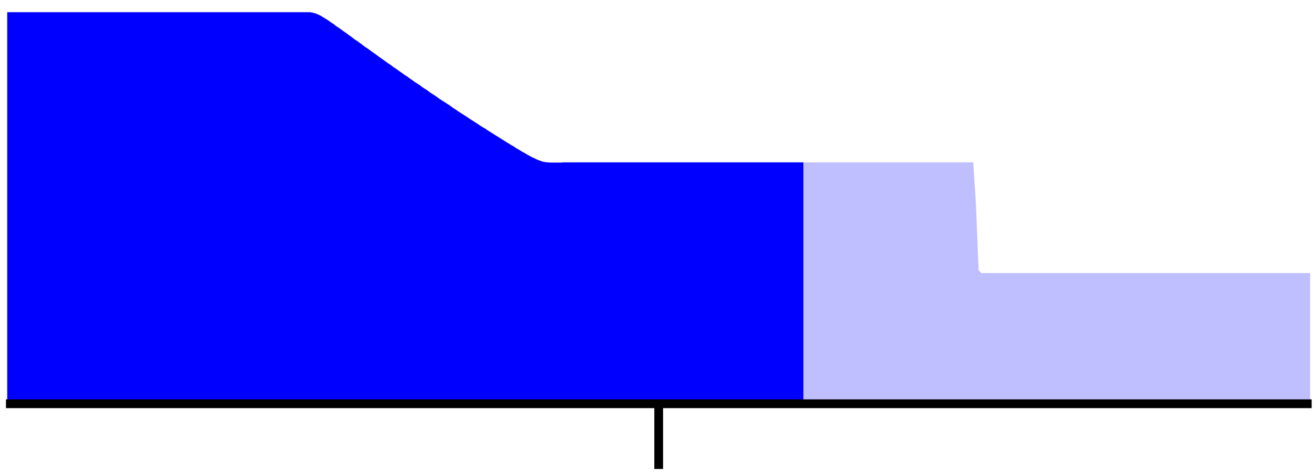

The Riemann problem

The Riemann problem for $q_t + f(q)_x = 0$ has special initial data

$$q(x,0) = \begin{cases} q_l & \text{if } x < x_{i-1/2} \\ q_r & \text{if } x > x_{i-1/2} \end{cases}$$

Dam break problem for shallow water equations

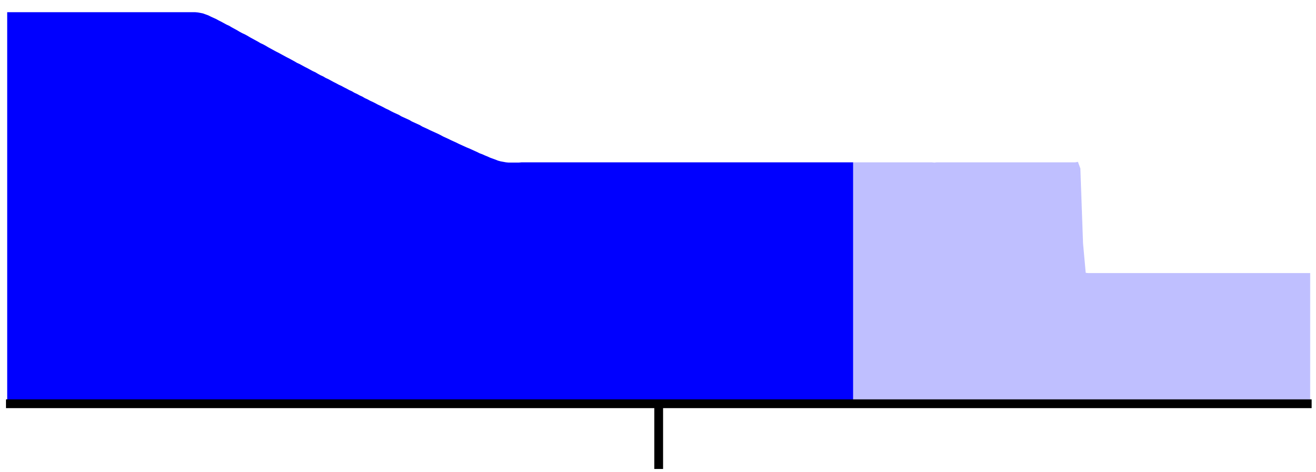

Riemann solution for the SW equations

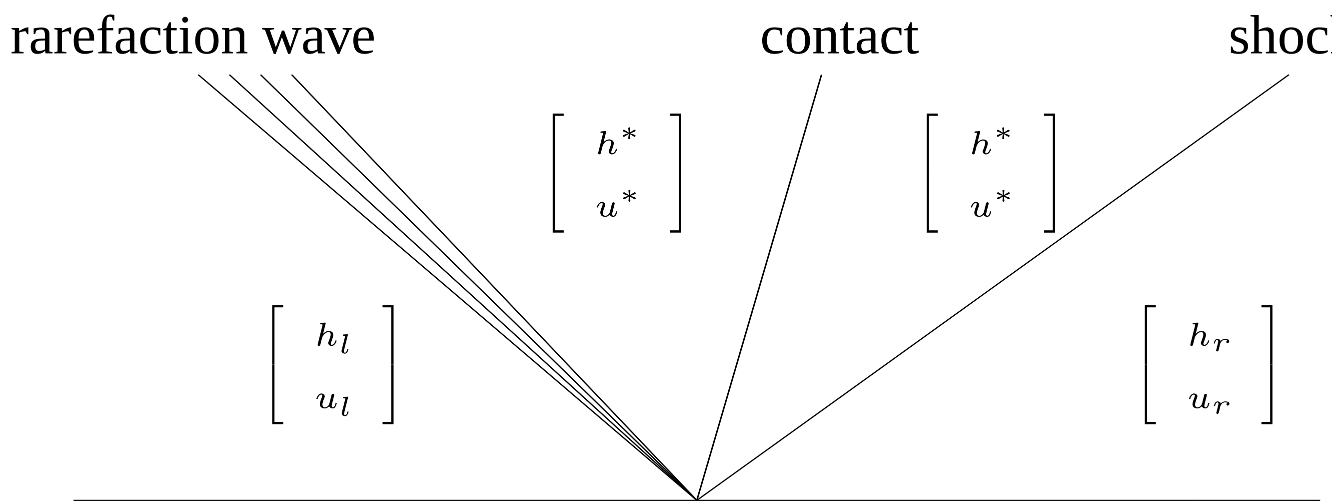

Godunov's method

Q_i^n defines a piecewise constant function

$$\tilde{q}^n(x, t_n) = Q_i^n \text{ for } x_{i-1/2} < x < x_{i+1/2}$$

Discontinuities at cell interfaces $\Longrightarrow$ Riemann problems.

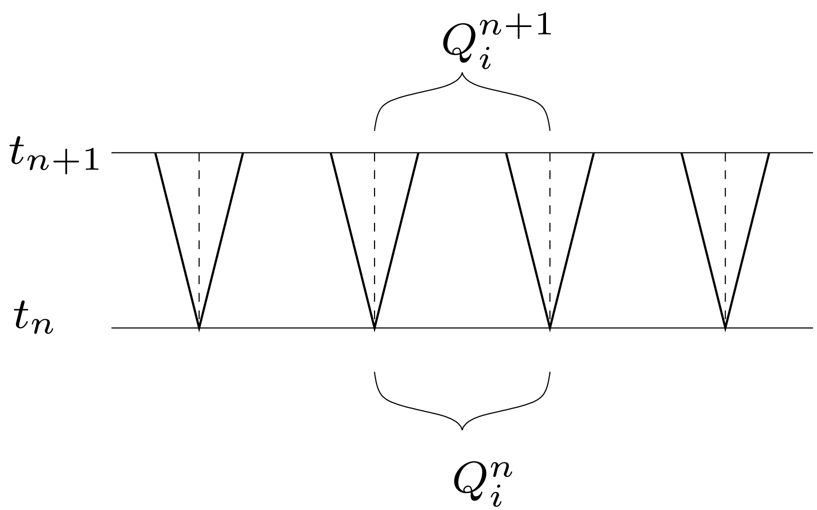

$$\tilde{q}^n(x_{i-1/2}, t) \equiv q^{\Downarrow}(Q_{i-1}, Q_i) \quad \text{for } t > t_n.$$

$$F_{i-1/2}^n = \frac{1}{\Delta t} \int_{t_n}^{t_{n+1}} f(q^{\Downarrow}(Q_{i-1}^n, Q_i^n))\, dt = f(q^{\Downarrow}(Q_{i-1}^n, Q_i^n)).$$

Riemann solution for the SW equations

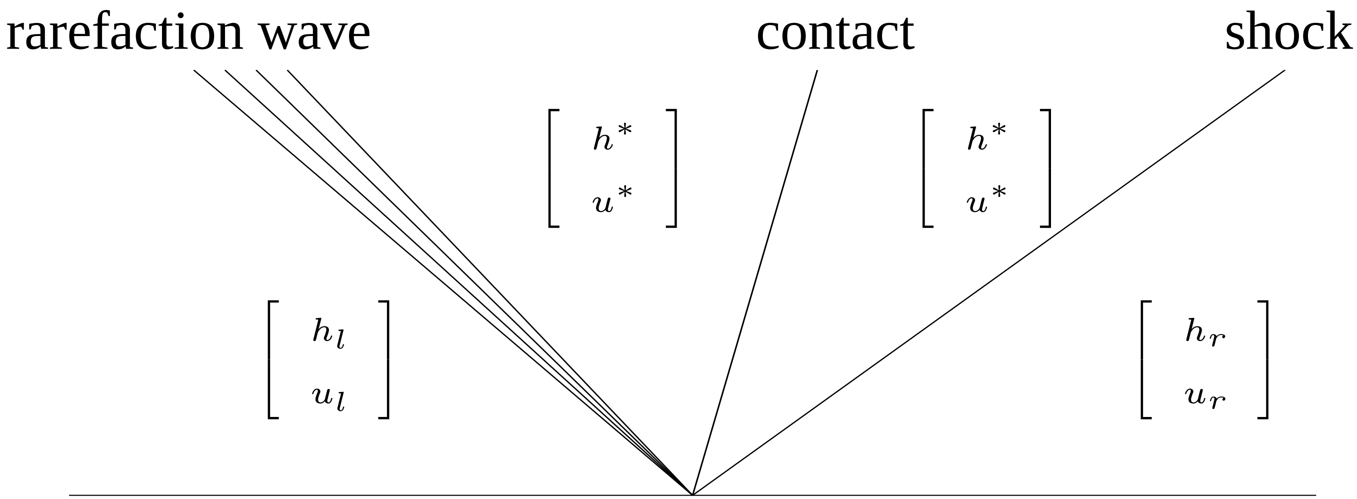

The Roe solver uses the solution to a linear system

$$q_t + \hat{A}_{i-1/2} q_x = 0, \qquad \hat{A}_{i-1/2} = f'(q_{\text{ave}}).$$

All waves are simply discontinuities.

Typically a fine approximation if jumps are approximately correct.

Wave decomposition for shallow water

$$q = \begin{bmatrix} h \\ hu \end{bmatrix}, \qquad f(q) = \begin{bmatrix} hu \\ hu^2 + \frac{1}{2}gh^2 \end{bmatrix}$$

Jacobian: $f'(q) = \begin{bmatrix} 0 & 1 \\ gh - u^2 & 2u \end{bmatrix}$

Eigenvalues: $\lambda^1 = u - \sqrt{gh}, \qquad \lambda^2 = u + \sqrt{gh},$

Eigenvectors: $r^1 = \begin{bmatrix} 1 \\ u - \sqrt{gh} \end{bmatrix}, \quad r^2 = \begin{bmatrix} 1 \\ u + \sqrt{gh} \end{bmatrix}$

Wave decomposition:

$$Q_i - Q_{i-1} = \sum_{p=1}^{m} \alpha_{i-1/2}^p r^p \equiv \sum_{p=1}^{m} \mathcal{W}_{i-1/2}^p.$$

Challenges for tsunami modeling

Want robust method with high resolution corrections that "captures" moving shoreline location

Need robust dry state Riemann solver

Modified HLLE solver that avoids negative h

Bottom bathymetry / topography

Source term incorporated into Riemann solver

f-wave formulation for $q_t + f(q)_x = \psi(q)$:

Split $f(Q_i) - f(Q_{i-1}) - \Delta x \Psi_{i-1/2} = \sum_p \beta^p_{i-1/2} r^p_{i-1/2}$

Wave-propagation viewpoint

For linear system $q_t + Aq_x = 0$, the Riemann solution consists of waves $\mathcal{W}^p$ propagating at constant speed s^p.

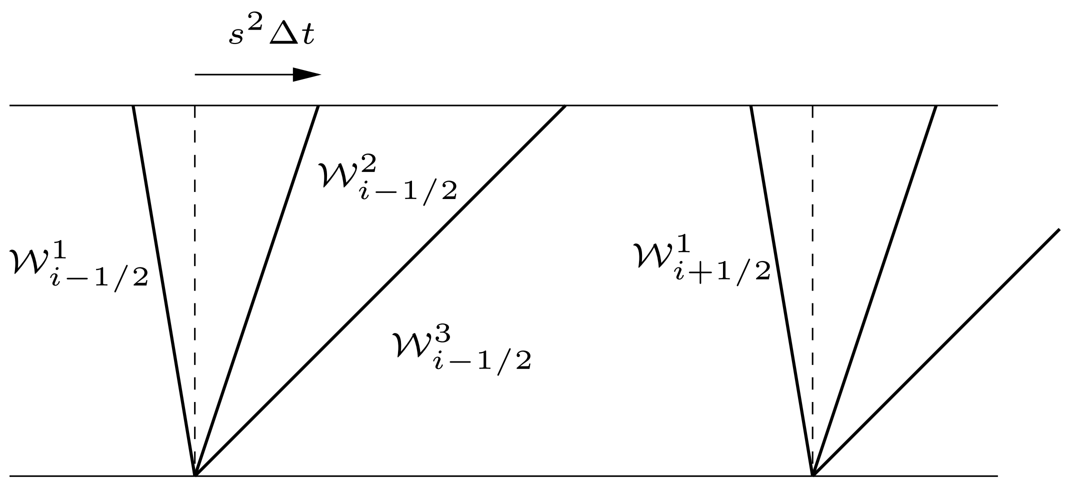

$$Q_i - Q_{i-1} = \sum_{p=1}^{m} \alpha^p_{i-1/2} r^p \equiv \sum_{p=1}^{m} \mathcal{W}^p_{i-1/2}.$$

$$Q_i^{n+1} = Q_i^n - \frac{\Delta t}{\Delta x}\left[s^2\mathcal{W}^2_{i-1/2} + s^3\mathcal{W}^3_{i-1/2} + s^1\mathcal{W}^1_{i+1/2}\right].$$

Upwind wave-propagation algorithm

$$Q_i^{n+1} = Q_i^n - \frac{\Delta t}{\Delta x}\left[\sum_{p=1}^{m}(s_{i-1/2}^p)^+\mathcal{W}_{i-1/2}^p + \sum_{p=1}^{m}(s_{i+1/2}^p)^-\mathcal{W}_{i+1/2}^p\right]$$

where

$$s^+ = \max(s,0), \qquad s^- = \min(s,0).$$

Note: Requires only waves and speeds.

Applicable also to hyperbolic problems not in conservation form.

Conservative if waves chosen properly,
e.g. using Roe-average of Jacobians.

Great for general software, but only first-order accurate (upwind).

Wave-propagation form of high-resolution method

$$Q_i^{n+1} = Q_i^n - \frac{\Delta t}{\Delta x}\left[\sum_{p=1}^{m}(s_{i-1/2}^p)^+\mathcal{W}_{i-1/2}^p + \sum_{p=1}^{m}(s_{i+1/2}^p)^-\mathcal{W}_{i+1/2}^p\right]$$
$$- \frac{\Delta t}{\Delta x}(\tilde{F}_{i+1/2} - \tilde{F}_{i-1/2})$$

Correction flux:

$$\tilde{F}_{i-1/2} = \frac{1}{2}\sum_{p=1}^{M_w}|s_{i-1/2}^p|\left(1 - \frac{\Delta t}{\Delta x}|s_{i-1/2}^p|\right)\tilde{\mathcal{W}}_{i-1/2}^p$$

where $\tilde{\mathcal{W}}_{i-1/2}^p$ is a limited version of $\mathcal{W}_{i-1/2}^p$.

CLAWPACK

`http://www.amath.washington.edu/~claw/`

- Fortran codes with Matlab graphics routines.
- Many examples and applications to run or modify.
- 1d, 2d, and 3d.
- Adaptive mesh refinement.

User supplies:

- Riemann solver, splitting data into waves and speeds
  (Need not be in conservation form)
- Boundary condition routine to extend data to ghost cells
  Standard `bc1.f` routine includes many standard BC's
- Initial conditions — `qinit.f`

Adaptive Mesh Refinement (AMR)

- Berger / Oliger / Colella
- Flag cells needing refinement
- Cluster into rectangular patches
- Refine in time also on patches
- Software:

  AMRCLAW (Berger, RJL)
  CHOMBO (Colella, et.al.)
  CHOMBO-CLAW (Calhoun)
  BEARCLAW (Mitran)
  AMROC (Deiterding)

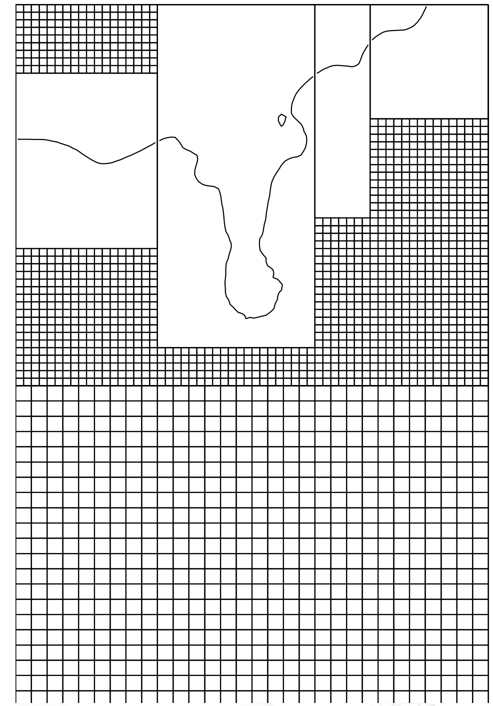

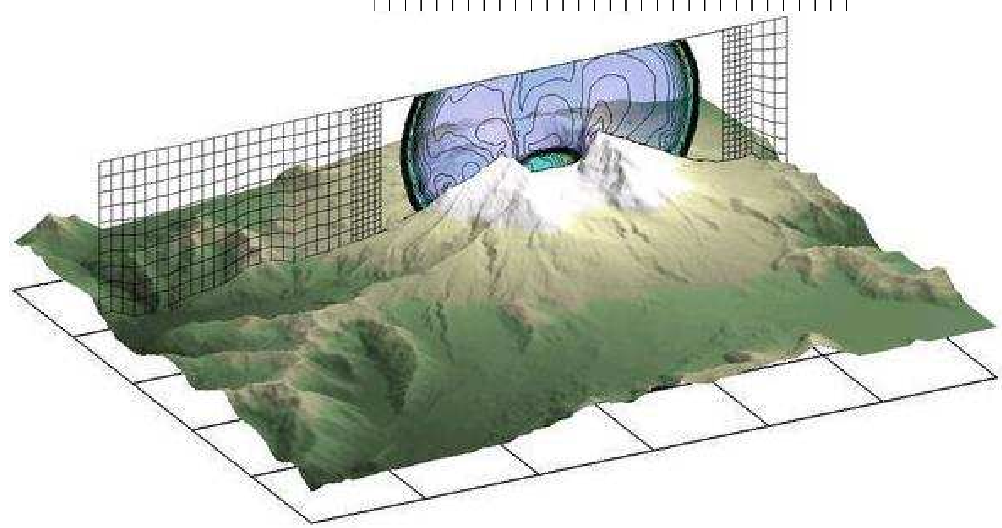

Some other applications

- Acoustics, ultrasound, seismology
- Elasticity, plasticity, soil liquifaction
- Flow in porous media, groundwater contamination
- Oil reservoir simulation
- Geophysical flow on the sphere
- Chemotaxis and pattern formation
- Multi-fluid, multi-phase flows, bubbly flow
- Streamfunction–vorticity form of incompressible flow
- Projection methods for incompressible flow
- Combustion, detonation waves
- Astrophysics: binary stars, planetary nebulae, jets
- Magnetohydrodynamics, plasmas
- Relativistic flow, black hole accretion
- Numerical relativity — gravitational waves, cosmology

Summary and extensions

- Applications to geophysical flows
- Scientific enquiry and hazard mitigation
- General formulation of high-resolution finite volume methods
- Applies to general conservation laws and nonconservative hyperbolic problems
- F-wave formulation for spatially varying fluxes and source terms
- Multi-dimensional extensions
- Adaptive mesh refinement
- CLAWPACK Software:

  `http://www.amath.washington.edu/~claw`